Design and Implementation of Analog Resonant Voltage Controller for Zero Voltage Switching Quasi Resonant Negative Output KY Boost Converter

S.Senthamil Selvan
Research Scholar, Department of Electrical and Electronic Engineering, SCSVMV University, Enathur, Kanchipuram, India
E-mail: sentamilselvans@gmail.com

R.Bensraj
Department of Electrical and Electronic Engineering, Annamalai University, Chidambaram, Tamilnadu, India
E-mail: bensraj_au@rediffmail.com

N.P.Subramaniam
Department of Electrical and Electronic Engineering, Pondicherry Engineering College, Pondicherry, India
Email:npsubbu@pec.edu

Abstract: *The negative output KY boost converter (NOKYBC) is one of the type dc-dc converters. It converts the conversion from +ve dc supply voltage into -ve dc load voltage. Owing to enhance the power capability and to minimize the size and weight of the magnetic and filter elements, the operating frequency of the dc-dc converter has to be improved. This article presents the analysis, design and output voltage control of a zero-voltage-switching quasi resonant-negative output KY boost converter (ZVS QR-NOKYBC) in continuous conduction mode (CCM). It works with reduced switching losses and suitable for applications needing the regulated power source such as various medical equipments, telecommunication systems, computer peripheral device, mobile phones etc. The simple control method analogue resonant controller UC3861 is utilized for ZVS QR-NOKYBC to stabilize the output voltage during the line, load variations, and also improve the power capability. The UC3861 controller performance is validated by building both an experimental and MATLAB/Simulink models of the proposed converter at various operating conditions. The results are indicated that the developed controller has excellent performance at different working regions.*

Key word: *DC-DC power conversion, zero voltage switching, negative output KY boost converter, analogue resonant controller IC UC3861.*

1. Introduction

In recent decades, the dc–dc power converters play a vital role in field of communication network, automobile phones, computer system, robot system and aerospace telemetry uses. The acceptable size and weight are awfully restricted to accommodate larger payload in aerospace utilization [1-4]. Owing to enhance the power capability and to minimize the size and weight of the magnetic and filter elements, the operating frequency of the dc-dc converter has to be improved. The negative output KY boost converter (NOKYBC) is one of the type dc-dc converters. It converts the conversion from +ve dc supply voltage into -ve dc load voltage [5-6]. The NOKYBC has the merits of simple circuit structure, large voltage gain, huge power capability, good efficiency and small output voltage/inductor current ripples over the traditional dc-dc converters as well as the Cuk and Luo-Coverters [7-12]. In general, the NOKYBC has multifaceted non-linear system with parameters modification. The reasonably better type in the topology of dc-dc converters, the NOKYBC, is chosen in this study. Generally, the power dc-dc converters working at high frequencies produce the large switching losses, decreased reliability and electromagnetic intervention. Owing to rectify the above pointed-out problems, quasi resonant converters (QRCs) are adopted in the NOKYBC. Increased power capability and efficiency will be determined using these converters for the reason that the turn-off takes

place either in zero current switching (ZCS) and in zero voltage switching (ZVS) [13].

In order to increase the recital of the power dc–dc converters, in particular the efficiency, it is essential to apply the ZVS and the ZCS resonant switching methods. The typical dc-dc converter based system must have a well tuned feedback controller for the load voltage control under the line and load disturbances. Owing to increase the quick settling of output response and near attain better voltage control, it is essential to have a feedback-loop regulation operation of the model. The simulation and implementation of output voltage regulation of QRCs using proportional–integral–derivative (PID) controller design based on the state space average modelling has been addressed in [14]. Boost power converter has been designed for a load voltage control [15]. The small signal model analysis and modeling of buck and super lift Luo-converters have been presented [16]. The above mentioned systems are sensitive to both the various operating conditions as well as the circuit components variations. In addition, the output voltage control is obtained with help of analog proportional integral controller (PIC) and operating gating pulses are produced through the analog platform pulse producing circuits. Also, a driver unit is applied to force the power switches. Moreover, individual sources were required to turn on the networks, which results in improve the size and weight of the presented converter, which are solved by using an enthusiastic analog integrated circuit (IC) UC3861 controller for load voltage control. Sliding mode controller and posicast controller for dc-dc power converters has been addressed in [17-18]. The application of analog resonant controller to fixed frequency various types dc-dc converters using ZVS-QRC has been reported [19-26].

In this paper, it is proposed to design and regulate the output voltage of zero voltage switching quasi-resonant negative output KY boost converter (ZVS QR-NOKYBC) operated in continuous conduction mode (CCM) using single IC UC3861 controller. Moreover, the performance of the designed converter is validated for line and load disturbances. The organization of the paper is as follows. The analysis and modes of operation of ZVS QR-NOKYBC presents in section 2. The dc voltage conversion ratio of ZVS QR-NOKYBC is executed in section 3. Development of ZVS QR-NOKYBC is reported in section 4. The results of the developed converter using analog resonant controller is well addressed in section 5. The conclusions are listed in section 6.

2. Analysis and states of working of ZVS QR-NOKYBC

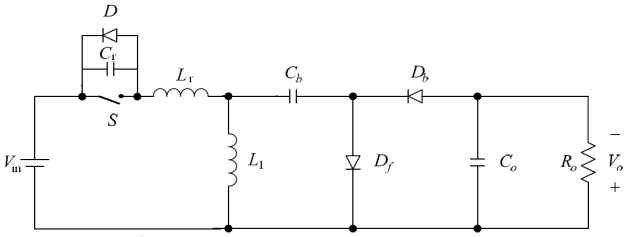

Fig.1. Circuit diagram of proposed converter.

The power circuit diagram of proposed converter (ZVS QR-NOKYBC) is depicting in Fig. 1. It consists of a power switch S, inductor L_1, one freewheeling diode D_b, R is load resistance, one output capacitor C_o and one energy transferring capacitors C_b with energy transferring diode D_b. The resonant capacitor C_r and resonant inductor L_r form a circuit. Duty ratio is k, switching frequency is f_s (period $T_s = 1/f_s$) and the load resistance is a R_0. The input voltage and input current are V_{in} and I_{in}. Load voltage and load current are V_0 and I_0. The voltage transfer gain is $M = V_0/V_{in}$. The following conditions are made as assumptions to analyze the constant-state characteristic of the ZVS QR-NOKYBC operating in CCM:

- Power switches are ideal,
- Reactive components in the circuit are ideal,
- Inductor L_1 are higher than resonating inductor L_r, and
- The load capacitor C_O and the load resistance R_0 are a stable sink of load current I_0.

To investigate the constant-state characteristic of designed converter, each switching period is alienated into four states of working. I_M, i_{Lr} , v_{Cr} and Z_0 are

respectively the magnetizing current, the resonant inductor current, the resonant capacitor voltage and the characteristic impedance. The equivalent circuit diagram for each state and the numerical waveforms of resonant capacitor voltage and inductor current are illustrated in Figs. 2 and 3, respectively.

2.1 States of working

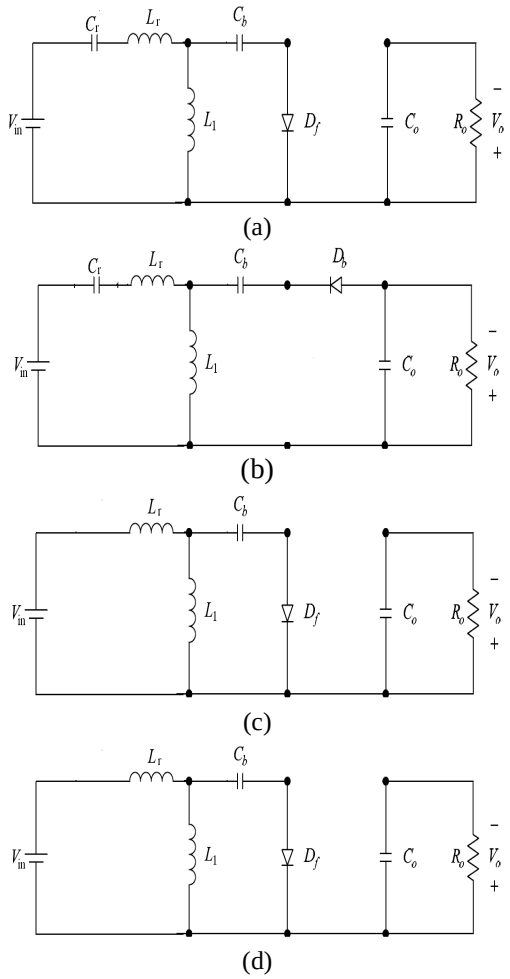

Fig.2. Equivalent circuit diagram of a ZVS QR-NOKYBC in four topological states of a switching cycle, (a) state I - $t_o \le t \le t_1$, (b) state II – $t_1 \le t \le t_2$, (c) state III – $t_2 \le t \le t_3$, and (d) state IV – $t_3 \le t \le t_4$.

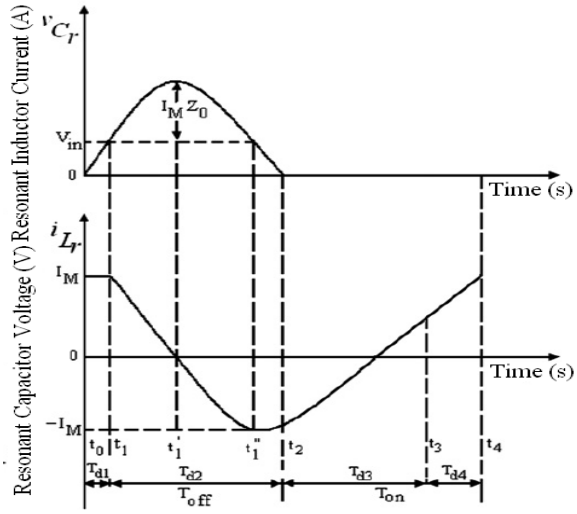

Fig.3. Numerical resonant waveforms of the designed converter.

2.1.1 State I: $t_o \le t \le t_1$: State I is initiated at $t=t_o$, when the power switch S is in open condition under ZVS state and the diode D is in closed state. The equivalent circuit of this state is exposed in Fig. 2(a). For the duration of this state, the v_{cr} increases linearly with slope I_M/C_r, which is always smaller than V_{in}. This is called as the voltage linear rising interval. Then, the mathematical relation of $V_{cr}(t)$ and inductor current i_{Lr} (t) are expressed as (1) and (2)

$$v_{Cr}(t) = \frac{I_M t}{C_r} \tag{1}$$

$$i_L(t) = I_M \tag{2}$$

On $t=t_1$, the $V_{cr}(t)$ reaches V_{in}. The period of this state is engraved by

$$T_{d1} = \frac{C_r V_{in}}{I_M} \tag{3}$$

2.1.2 State II: $t_1 \le t \le t_2$: In this state, since i_{Lr} starts decreasing, the diode D_f is reverse biased and hence it is non-conduction state. The equivalent circuit of this state is revealed in Fig. 2 (b). During this state, as the

power switch S remains in open state, the storage components L_r and C_r form a series resonant circuit. This is known as the resonance interval as shown in Fig. 3. The state equations are

$$C_r \frac{dv_{Cr}}{dt} = i_{Lr}(t) \quad (4)$$

$$L_r \frac{di_{Lr}}{dt} = V_{in} - v_{Cr}(t) \quad (5)$$

With initial condition $v_{Cr}(t1)=V_{in}$ and $i_{Lr}(t1)=I_M$. The solutions of the state equation are

$$v_{Cr}(t) = V_{in} + I_M Z_o \sin \omega_o t \quad (6)$$

$$i_{Lr}(t) = I_M \cos \omega_o t \quad (7)$$

$$\text{Where, } \omega_o = \frac{1}{\sqrt{L_r C_r}}$$

While the current through L_r starts falling, it causes a raise in v_{Cr} and at time $t=t_1$, the current i_{Lr} touches null and v_{cr} reaches the peak value.

$$v_{Cr}(t_1') = V_{Cr-peak} = V_{in} + I_M Z_o \quad (8)$$

$$i_{Lr}(t_1') = 0 \quad (9)$$

The I_M could reach a high values with condition $I_M Z_O > V_{in}$ in the ZVS state. If conditions are not obeyed, the voltage across the switch can not arrive back to null naturally, resulting in turn-ON loss. During the period $t'_1 \le t \le t''_1$, the energy is transferred from C_r back to L_r, v_{Cr} is decreasing from its peak value to V_{in} and i_{Lr} reaches the negative peak of I_M. On $t = t_2$, the solutions of (4) and (5) with initial condition $v_{Cr}(t''_1) = V_{in}$ and $i_{Lr}(t''_1) = -I_M$ are expressed by

$$v_{Cr}(t_1'') = V_{in} + -_M Z_o \sin \omega_o t \quad (10)$$

$$i_{Lr}(t_1'') = -I_M \cos \omega_o t \quad (11)$$

At $t=t_2$, the v_{Cr} reaches zero, to achieve ZVS for "S".

$$v_{Cr}(t_2) = 0 \quad (12)$$

$$i_{Lr}(t_2) = -I_M \cos \alpha \quad (13)$$

Where, $\alpha = \sin^{-1}(V_{in}/I_m Z_o)$

Time period for this state is expressed as (14)

$$T_{d2} = t_2 - t_1 = \left(\frac{\pi + \alpha}{\omega_o} \right) \quad (14)$$

2.1.3 State III: $t_2 \le t \le t_3$: During this period, the S is in closed state at $t= t_2$ to accomplish ZVS condition. The equivalent circuit of this state is indicated in Fig. 2(c). The diode, D don't allow the V_{Cr} to become a negative value. The current, i_{Lr} increases linearly with an incline slope of V_{in}/L_r. This is called as the linear recovering interval as shown in Fig.3, because the I_o is a stable current and the i_{Lr} increase linearly from $-I_m\cos\alpha$ to 0 on $t= t_3$. The time period of this state is given by

$$T_{d3} = \frac{2(I_M \cos \alpha) L_r}{V_{in}} \quad (15)$$

2.1.4 State IV: $t_3 \le t \le t_4$: The equivalent circuit diagram of this state is depicted in Fig. 2(d). In this period, the I_o is supplied by the source. The "S" is in conduction state till time of $t + t_4$. This is known as the normal switch on interval. During this state, i_{Lr} rises from 0 to I_M. This state continues till the "S" is opened at time of $t=t_4$ and the cycle repeats. The time period of this state is expressed as (16)

$$T_{d4} = T_s - \left(T_{d1} + T_{d2} + T_{d3} \right) \quad (16)$$

3. DC voltage conversion ratio of proposed converter

In an ideal state, over a switching period, input energy E_{in} is equal to the output energy E_o (from the conversion of energy theory).

$$E_{in} = V_{in} \left(\int_0^{\frac{T_{d1}}{2}} i_{Lr}(t)\,dt + \int_0^{T_{d4}} i_{Lr}(t)\,dt \right) \quad (17)$$

$$E_o = V_o I_o T_s \quad (18)$$

Next, the dc voltage conversion ratio of the designed converter is defined by (19).

$$M = \frac{V_o}{V_{in}} = \frac{1}{T_s}\frac{I_M}{I_o}(T_s - \frac{T_{d1}}{2} - T_{d2} - T_{d3}) \quad (19)$$

By substituting the values of T_{d1}-T_{d3}, (19) is modified and engraved in terms of circuit parameters as

$$M = \frac{I_M}{I_o}\left[1 - \frac{I_o C_r f_s R_o}{2MI_M} - \frac{\pi + \alpha}{2\pi} * \frac{f_s}{f_o} + \frac{2(I_M \cos\alpha)L_r f_s}{V_{in}}\right] \quad (20)$$

Table 1.Voltage conversion ratio (M) for various normalized switching frequencies with various load resistance

f_{ns}	Voltage conversion ratio (M)	
	@ R= 125 Ω	@ R= 150 Ω
0.3205	9.49	9.46
0.2884	9.37	9.31
0.2564	9.21	9.15
0.2243	9.05	9.00

Where,

Resonant frequency $f_o = \frac{1}{2\pi\sqrt{L_r C_r}}$ (21)

Normalized operating frequency $f_{ns} = \frac{f_s}{f_o}$ (22)

Typical impedance $Z_o = \sqrt{\frac{L_r}{C_r}}$ (23)

Standardized load resistance $R = \frac{R_o}{Z_o}$ (24)

It is clearly showed that, M is a function of R_o and f_s. The value of M can be controlled by varying switching frequency. Voltage conversion ratio (M) for different normalized switching frequency (f_{ns}) and load (R) is given in Table 1. At R=150, M is 9.46 for f_{ns} of 0.3205. When R is varied from 150 to 125, M is increased from 9.47 to 9.49. To maintain the M at 9.47, f_{ns} has to be varied from 0.2243 to 0.3205. It is found that the variation of M with f_{ns} is almost linear and M is responsive to the R changes. Therefore, a feed back-loop regulation is needed to control the output voltage.

4. Design of ZVS QR-NOKYBC

This section discusses regarding the design specifications calculation of the designed converter. The specification of the designed converter is listed in Table 2.

Table 2.Specifications of the ZVS QR-NOKYBC

Parameters name	Symbol	Value
Input Voltage	V_{in}	12V
Output Voltage	V_o	-30V
Inductor	L_1	10µH
Capacitors	C_b, C_o	10 µF, 30 µF
Nominal switching frequency	f	100kHz
Load resistance	R_o	50Ω
Output power	P_o	18W
Input power	P_{in}	21W
Average input current	I_{in}	1.75A
Efficiency	η	85.78%
Average output current	I_o	-0.6 A
Duty ratio	d	0.6
Peak to Peak Inductor Current Ripple	Δ_{iL1}	25% of I_{in}
Peak to Peak Output Capacitor Ripple Voltage	ΔV_o	-0.18V

The magnetizing current is given by

$$I_M = (1 + M_{\max})I_o \quad (25)$$

Where, M_{max} is the largest value of voltage conversion ratio.

The state for ZVS is

$$I_M Z_o \succ V_{in} \quad (26)$$

To assure (26), choosing Z_0 = 10 ohm, normalized frequency f_{ns} = 0.3205 and resonant frequency f_0 = 312 kHz, the switching frequency (f_s) and resonant

components (L_r and C_r) are evaluated using eqns (21) to (23) as 100 kHz, 5.2 uH and 0.05 uF, respectively.

5. Simulation and Experimental Results

The main function this part to argue on the simulation and experimental results of ZVS QR-NOKYC with designed control scheme.

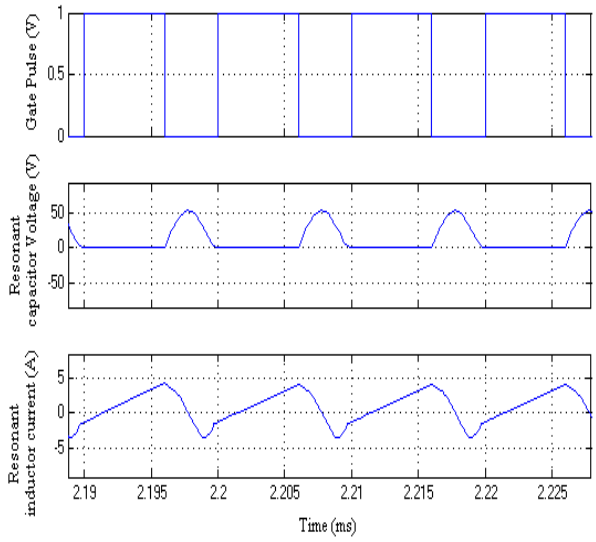

Fig.4. Simulated waveforms of resonant components

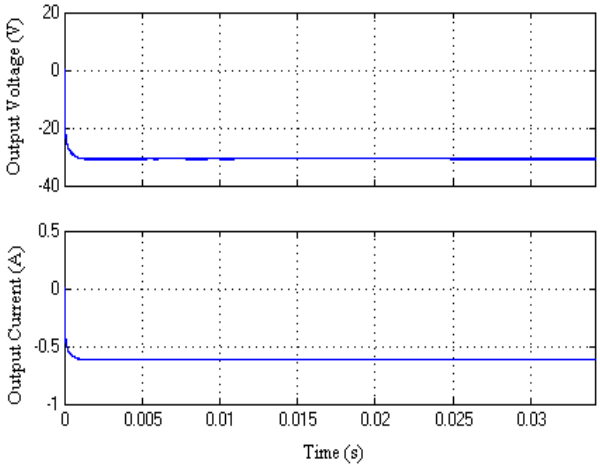

Fig.5. Simulated output voltage and current results of ZVS QR-NOKYBC.

The ZVS QR-NOKYBC is simulated using MATLAB/Simulink with the designed specifications (refer the end of the previous section). The simulated results of gate pulse, resonant capacitor voltage and inductor current, are depict in Fig. 4. From this figure, it is clearly found that the power switch S is in closed state, when the voltage across resonant capacitor befalls zero, in that way it suppresses the switching losses. The simulated results match very closely with the theoretical results shown in Fig. 3. A typical case is indicated in Fig. 5, where the developed converter functions for the rated load voltage and load current in open loop mode.

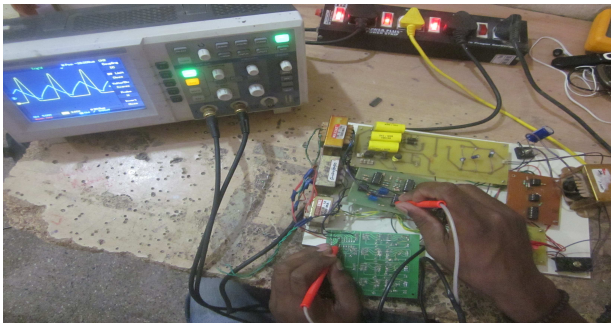

Fig.6. Experimental set-up of ZVS QR-NOKYBC using designed controller.

The experimental model of the ZVS QR-NOKYBC is implemented with the same simulation specification. The laboratory prototype model of ZVS QR-NOKYC using controller is shown in Fig.6. The parameters of the power circuits are as follows:

Q IRFN 540 (MOSFET);
D_b, D_f FR306 (Diodes);
C_b, C_O 30 µF/100V (Electrolytic and plain polyester type);
C_r 0.05 µF/100V (plain polyester type);
L_1 10µH/10A (Ferrite Core);
L_r 5.2µH/10A (Ferrite Core).

Fig. 7 (a) to Fig. 7(d) indicate the practical results of resonant capacitor voltage in the overlap of resonant inductor current, resonant capacitor voltage in the overlap of gate pulse, output current with output voltage and input voltage with output voltage . It is

found that the “S” is in closed exactly when the resonant capacitor voltage turns into zero to guarantee the ZVS condition. This result matches the simulated results as shown in Fig. 4. The minimal deviations obtain between the simulation and experimental results due to parasitic components. In addition, the feedback control of the ZVS QR-NOKYBC is essential to regulate the output voltage under line and load variations.

The circuit arrangement of the proposed converter is shown in Fig. 8. In this article, analogue resonant controller (UC3861) is employed for load voltage regulation of the designed converter. For feedback operation, the load voltage is measured and fed through an opto-coupler (6N137) to the non-inverting terminal of IC UC3861 (at pin no. 2). The function of opto-coupler is to isolate between the power circuit and controller circuit. The power supply for the opto-coupler is utilized from the 5V pin of UC3861 (pin no.1) and the additional source requirement is avoided.

Soft-reference of the controller IC (at pin no. 16) is set as the system reference signal, which is connected to the inverting terminal of control IC (UC3861 at pin no. 3). The resonant capacitor voltage is applied to the zero pin of IC UC3861 (at pin no.10) through 6N137 opto-coupler to reach the ZVS state. The R_{range} (at pin no. 6), R_{min} (at pin no. 7) and Cvco (at pin no. 8) are connected respectively to be 25 kΩ (resistance), 200 kΩ (resistance) and 1 nF (capacitance). These values are computed for the voltage-controller oscillator frequency between 21kHz to 148 kHz. The output of the oscillator acts as the internal clock and is applied to trigger the one-shot timing generator. The one shot generator modulates the pulse width of the gate signal depending on the zero crossing of v_{Cr}. The output driver of controller IC (at pin no. 11) is straightly connected to the gate of the MOSFET IRF540 through a resister of 100Ω as marked in Fig. 8. The operating frequency of the gate pulse is altered to regulate the load voltage with help of the controller IC. In feedback-loop operation, the controller IC is proficient to keep the load voltage equal to the set reference output voltage value of -30V when variation in supply voltage of 3.5V and the output voltage waveform is represented in Fig.9 (a).

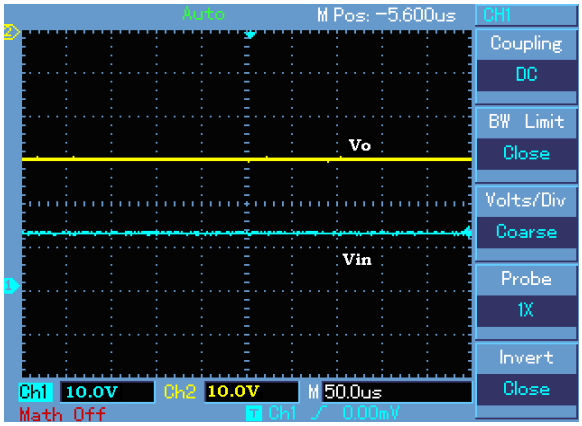

Fig.7. Open loop experimental results of ZVS QR-NOKYBC using designed controller, (a) resonant capacitor voltage and resonant inductor current, (b) resonant capacitor voltage and gate pulse, (c) output voltage and load current, and (d) output voltage and input voltage [Ch1:1A/Div -output current and Ch2:10V/Div- input voltage, output voltage, and resonant capacitor voltage].

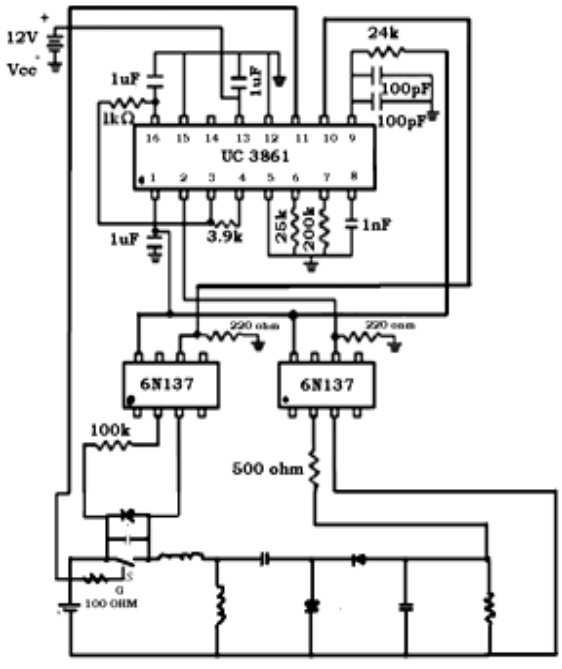

Fig.8. Circuit arrangement of closed loop control of ZVS QR-NOKYBC using UC3861

The controller IC performs effectively and brings back the load voltage to the reference value of -30 V for 20% load resistance disturbance as evidenced in Fig. 9(b). From these results, it is clearly observed the merits and the suitability of the controller IC for the load voltage control in the designed converter. Fig.10 shows the efficiency of the designed converter at different values of output currents. With efficiencies surpassing over 94%, the converter outperforms.

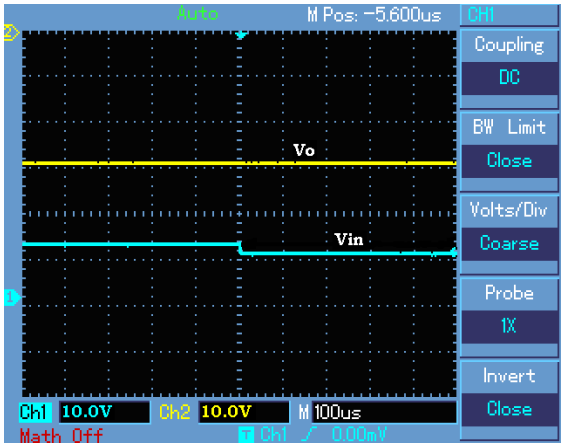

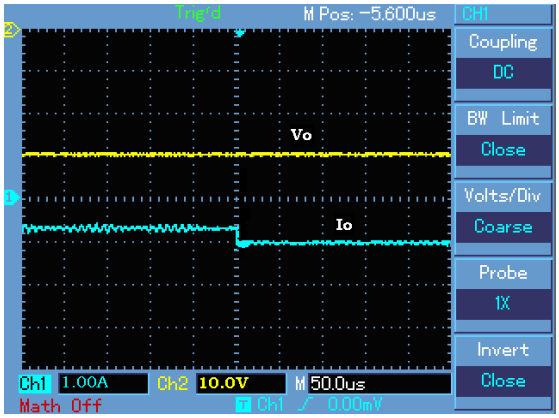

Fig.9. Closed loop experimental results of ZVS QR-NOKYBC using designed controller at line and load variations, (a) output voltage and input voltage and, (b) output voltage and output current [Ch1:1A/Div -output current and Ch2:10V/Div- input voltage, output voltage].

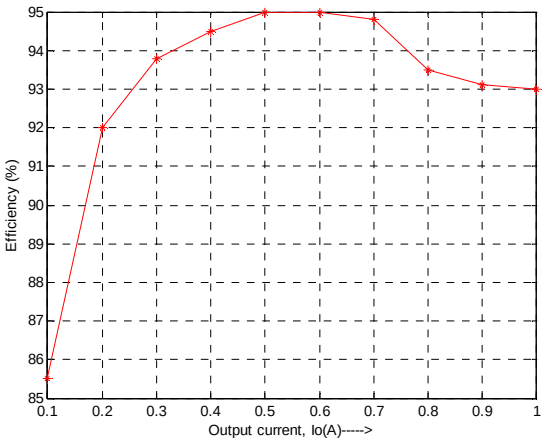

Fig.10. Efficiency of designed converter at 12V input

6. Conclusions

In this article, analysis, design, and output voltage regulation of the ZVS QR-NOKYBC operated in CCM with analogue resonant enthusiastic controller IC UC3861 are performed. Theoretical key results match with the simulated results. The results of both the experimental and simulations are offered to illustrate the success of designed controller for the proposed converters. The system effected in quick dynamic response, excellent regulated output voltage during the input supply voltage and load resistance variations, good steady state and initial start-up responses. The proposed converter with controller is, therefore, suitable for any constant low power source real-world commercial applications and it is mainly designed for power supply in different medical equipments, telecom, battery charging of solar power panels, industrial and military applications.

References

[1] Abutbuli, O., Gherlitz, A., Berkovich, Y., Ioinovici, A., "Step-up switching-mode converter with high voltage gain using a switched-capacitor circuit", *IEEE Transactions on Circuits Systems*. I 2003; 50, (8):1098−1102.

[2] R.M.Rashmi, A.Suresh, " A Four Port DC-DC Converter for Renewable Energy", Journal of Electrical Engineering, http://www.jee.ro/covers/art.php?issue=WK1322028973W4ecc8fad4d7f8.

[3] Tseng, C., Liang, T.J. Novel high-efficiency step-up converter. *IEE Proc. Electr. Power Appl.*, 2004; 151, (2):182−190.

[4] http:/www.researchandmarkets.com.

[5] K. I. Hwu and W. Z. Jiang, "Voltage Gain Enhancement for a Step-Up Converter Constructed by KY and Buck-Boost Converters", *IEEE Transactions on Industrial Electronics*, vol. 61, no. 4, pp. 1758-1768, April 2014.

[6] K. I. Hwu, W. C. Tu, and Y. H. Chen, A novel negative –output KY boost converter. *International conference on PEDS 2009*, pp. 1155-1157.

[7] Zhu. M., Luo.F.L. Implementing of developed voltage lift technique on SEPIC, CUK and double-output DC–DC converters. *IEEE Trans. Ind. Electron. Appl.*, 2007; 23, (25): 674–681.

[8] K. I. Hwu, W. Z. Jiang and J. J. Shieh, "Study and simulation on control-to-output transfer function of KY boost converter," *Industrial Electronics Society, IECON 2015 - 41st Annual Conference of the IEEE*, Yokohama, 2015, pp.146-149.

[9] Luo, F.L. Luo converters – voltage lift technique. *Proceedings of the IEEE Power Electronics Special Conference (PESC'98)*, Fukuoka, Japan, 1998: 17, (22):1783-1789.

[10] Luo, F.L. Positive output Luo-converters voltage lift technique. *IEE-EPA Proc*., 1999; 146, (4): 415–432.

[11] Luo,F., Ye, H. Positive output super lift converters. *IEEE Transaction on Power Electronics* 2003; 18, (1): 105-113.

[12] F.L.Luo and H.Ye. Negative output cascade boost converters. *IEE Proc.-Electr. Power Appl.*, September 2004; 151, (5):590-606.

[13] Rama Reddy .S, Chellamuthu .C, Analysis and design of a buck FM-ZCS-QRC fed DC drive. *AMSE J. Modeling (France)*, 1995, 6, (!). Pp.1-14.

[14] UMA G., Simulation and implementation of controlled quasi resonant converters. PhD thesis, Anna University, Madras, 2001.

[15] ZHU M., LUO F.L., Series SEPIC implementing voltage-lift technique for dc –dc power conversion. *IET Power Electron.*, 2008, 1, (1), pp. 109–121.

[16] Fang Lin Luo, Hong Ye, Energy factor and mathematical modeling for power DC-DC converters. *IEE Proc.-Electr. Power Appl.*, Vol.152, No. 2, March 2005, pp. 191-198.

[17] K. RamashKumar, S. Jeevananthan, Design of a Posicast Control for a DC-DC Boost Converter Operated in Continuous Conduction Mode. *Proceedings of ICETECT 2011*, 2011, p.240–248.

[18] K. RamashKumar, S. Jeevananthan, Design of Sliding Mode Control for Negative Output Elementary Super Lift Luo-Converter Operated in Continuous Conduction Mode. *International Conference on Communication Control and Computing Technologies* 2010, 2010, p.138–148.

[19] E. Jayashree G. Uma, Soft-switched-controlled-ultra lift Luo. *IET Power Electron*., 2011, Vol. 4, Iss. 1, pp. 151–158. 21.

[20] S.Arulselvi, G. Uma, 'Design and implementation of CF-ZVS-QRC using analog resonant controller UC3861. Int. J. Electron., 2007, 94, (1–2), pp. 55–73.

[21] E. Jayashree G. Uma, Simulation and implementation of quasi resonant-negative output converter. *International Journal of Power Electronics*, Vol.3, No.5, 2011, pp. 547–560.

[22] http:/www.waset.org.

[23] Texas Instruments, Resonant – mode power supply controllers. Application information, Unitrode products, slus289, October 1998.

[24] E.Jayashree and G.Uma, " Design and Implementation of Quasi Resonant- Negative Output Super Lift Luo Converter", Journal of Electrical Engineering, URL:http://www.jee.ro/covers/art.php?issue=WC12549 94386W4acdb1d2bbb84.

[25] S. Salehi Dobakhshari; J. Milimonfared; M. Taheri; H. Moradisizkoohi,"A quasi-resonant current-fed converter with minimum switching losses," *IEEE Transactions on Power Electronics* , vol.PP, no.99, pp.1-1.

[26] J. A. Taborda, P. P. Fajardo and F. F. Montes, "Control of buck quasi-resonant converter with delayed PWM scheme," *Power Electronics and Power Quality Applications (PEPQA), 2015 IEEE Workshop on*, Bogota, 2015, pp. 1-5.